Theoretical Study of Structure, Electronic Properties, and Photophysics of Cyano-Substituted Thiophenes and Terthiophenes

Roland Šolc,[†] Vladimír Lukeš,[*,†] Erik Klein,[†] Markus Griesser,[‡] and Anne-Marie Kelterer[‡]

Institute of Physical Chemistry and Chemical Physics, Slovak University of Technology in Bratislava, Radlinského 9, SK-812 37 Bratislava, Slovak Republic, and Institute of Physical and Theoretical Chemistry, Graz University of Technology, Technikerstrasse 4/I, A-8010 Graz, Austria

Received: June 26, 2008; Revised Manuscript Received: August 08, 2008

In this paper, quantum chemical calculations for various cyano derivatives of thiophene and terthiophenes at the density functional theory (DFT) and ab initio Møller–Plesset (MP2) levels of theory are presented. In the case of the studied terthiophenes, CN groups located in the central part of the molecule lead to a preference of cis–cis geometry over trans–trans conformation. For α-substituted dicyano terthiophene, the investigation of torsional dependences shows that the highest energy barrier occurs at the perpendicular orientation of the aromatic rings. On the other hand, the dicyano substitution in the central part of terthiophene molecule exhibits the lowest energy barrier. Excitation energies were calculated using time-dependent density functional theory (TD-DFT). The obtained theoretical results show that the CN groups in α and β positions have a distinct effect on the excitation energies and corresponding oscillator strengths. A CN group located in the α position causes a larger bathochromic shift than a CN group in the β position. Besides, a CN group in the β position has negligible influence on the position of the first absorption maximum.

1. Introduction

Compounds based on the thiophene aromatic ring are ubiquitous in nature.[1] Thiophene oligomers and polymers have received great attention due to their potential application in various electronic devices including organic light-emitting diodes (OLED) and field-effect transistors (FET).[2,3] Moreover, substituted thiophenes and their derivatives play a role in the synthesis of many biologically active compounds, photosensitizers for photodynamic therapy, insecticides, or in organometallic magnetic compounds.[4–6] Therefore, considerable effort is focused on understanding the electronic structure and photochemical properties of various thiophene derivatives.

The main advantage of the simple thiophene molecule or oligomers is their relatively well-defined molecular structure and chain lengths that allow determination of the structure–property relationships in detail. Oligomers with various numbers of monomer units enable the evaluation of the effect of increasing conjugation and the estimation of the properties of a polymer. Therefore, a large number of organic systems based on thiophene structural units was studied, both experimentally and theoretically.[7–12] Substitutions in the oligomeric chain can improve the solubility and lead to beneficial modifications of electro-optical properties.[13] Another way to tune photophysical properties is the introduction of other chromophors into the oligomeric chain.[14–16]

Cyano substitution plays a specific role in molecular modification techniques.[17] The strong electron-withdrawing CN group as a small substituent enables one to establish intermolecular contacts between the molecules in the solid state. Additionally, it leads to the arrangement of oligothiophene chains through intermolecular CN···H interactions. Cyano-oligothiophenes efficiently promote n-channel conduction in transistors.[18] With the use of in situ electrochemistry and various optical techniques, the redox properties and spectroscopic vibrational features were experimentally studied for large series of simple cyano-substituted oligothiophenes in their neutral and charged forms.[19] To explain the experimental results, various quantum chemical studies were presented.[20–22] However, a complex theoretical description of the electronic structure of cyano-substituted thiophenes and the description of the torsional potentials for terthiophene derivatives are still absent.

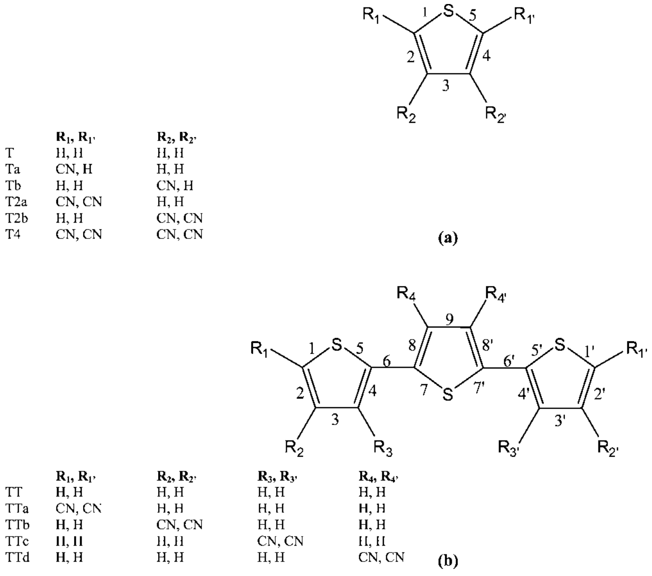

	$R_1, R_{1'}$	$R_2, R_{2'}$
T	H, H	H, H
Ta	CN, H	H, H
Tb	H, H	CN, H
T2a	CN, CN	H, H
T2b	H, H	CN, CN
T4	CN, CN	CN, CN

	$R_1, R_{1'}$	$R_2, R_{2'}$	$R_3, R_{3'}$	$R_4, R_{4'}$
TT	H, H	H, H	H, H	H, H
TTa	CN, CN	H, H	H, H	H, H
TTb	H, H	CN, CN	H, H	H, H
TTc	H, H	H, H	CN, CN	H, H
TTd	H, H	H, H	H, H	CN, CN

Figure 1. Bond numbering of the investigated thiophenes (a) and terthiophenes (b).

In this work, the attention will be focused on the quantum chemical calculation of model thiophene and terthiophene cyano derivatives (Figure 1). We have employed DFT (density functional theory)[23] and ab initio MP2 (Møller–Plesset pertur-

---

[*] Corresponding author. E-mail: vladimir.lukes@stuba.sk.

[†] Slovak University of Technology in Bratislava.

[‡] Graz University of Technology.

10.1021/jp805629u CCC: $40.75

TABLE 1: Optimum B3LYP/6-31G(d) and MP2/6-31G(d) Bond Lengths (in angstroms), Ionization Potentials (IP in eV), Dipole Moments (μ_0 in D), and Total Energies (E_{tot} in hartree) of the Thiophenes[a]

bond: (method)	1	2	3	4	5	IP	μ_0	BLA	E_{tot}
T:									
DFT/6-31G(d)	1.718	1.376	1.420	1.376	1.718	6.33	0.63 (0.55)	0.243	−553.002628
MP2/6-31G(d)	1.736	1.367	1.430	1.367	1.736	8.71	0.77 (0.70)	0.267	−551.288064
MP2/TZVP[b]	1.724	1.380	1.418	1.380	1.724		0.32	0.242	
exptl MW[c]	1.714	1.370	1.423	1.370	1.714			0.247	
exptl ED[d]	1.712	1.360	1.454	1.360	1.712			0.266	
exptl[e]							0.55		
exptl[f]							0.54		
exptl[g]						8.80			
exptl[h]						8.85			
T1a:									
DFT/6-31G(d)	1.715	1.379	1.413	1.386	1.728	6.96	4.75 (4.92)	0.236	−645.245042
MP2/6-31G(d)	1.723	1.371	1.420	1.379	1.751	9.34	5.23 (5.30)	0.256	−643.938029
exptl[i]						9.83			
T1b:									
DFT/6-31G(d)	1.717	1.374	1.425	1.384	1.709	7.09	4.09 (4.37)	0.238	−645.245950
MP2/6-31G(d)	1.737	1.363	1.437	1.378	1.723	9.49	4.34 (4.49)	0.262	−643.939085
T2a:									
DFT/6-31G(d)	1.726	1.389	1.405	1.389	1.726	7.50	2.50 (2.54)	0.230	−737.482463
MP2/6-31G(d)	1.744	1.382	1.413	1.382	1.744	9.86	2.94 (2.95)	0.252	−735.947116
exptl[j]						9.76			
T2b:									
DFT/6-31G(d)	1.709	1.382	1.432	1.382	1.709	7.74	6.46 (6.85)	0.235	−737.482523
MP2/6-31G(d)	1.724	1.374	1.447	1.374	1.724	10.14	7.05 (7.26)	0.258	−735.947344
exptl[j]						10.20			
T4:									
DFT/6-31G(d)	1.722	1.395	1.421	1.395	1.722	8.83	3.79 (4.01)	0.227	−553.002628
MP2/6-31G(d)	1.737	1.389	1.433	1.389	1.737	10.83	4.11 (4.21)	0.247	−551.924982

[a] See Figure 1a for bond notation. Values in parentheses represent the B3LYP/6-31+G(d)//B3LYP/6-31G(d) calculations. [b] Ref 34. [c] Ref 32. [d] Ref 33. [e] Ref 36. [f] Ref 37. [g] Ref 38. [h] Ref 39. [i] Ref 40. [j] Ref 41.

TABLE 2: Theoretical Excitation Energies (in eV) and Oscillator Strengths $f > 0.01$ (in Parentheses) of the First Three Dominant Electronically Excited States of the Thiophenes

molecule	TD-B3LYP/6-31+G(d)	TD-B3LYP/6-31G(d)	TD-B3LYP/3-21G*	experiment
T	5.73 (0.102)	5.93 (0.087)	6.11 (0.085)	in THF: 5.39[a]
	5.81 (0.090)	6.00 (0.082)	6.12 (0.090)	in acetontrile: 5.37[b]
	6.65 (0.023)	7.97 (0.210)	8.20 (0.188)	
T1a	4.97 (0.226)	5.08 (0.206)	5.25 (0.197)	in ethanol: 4.76, 5.12[c]
	5.37 (0.101)	5.48 (0.093)	5.63 (0.101)	
	6.90 (0.071)	7.01 (0.017)	7.24 (0.025)	
T1b	5.38 (0.043)	5.48 (0.051)	5.64 (0.080)	in hexane: 5.25, 5.51[d]
	5.44 (0.148)	5.56 (0.132)	5.74 (0.102)	
	6.45 (0.305)	7.18 (0.122)	6.84 (0.235)	
T2a	4.51 (0.391)	4.59 (0.367)	4.76 (0.355)	
	4.98 (0.066)	5.06 (0.060)	5.19 (0.064)	
		6.68 (0.147)	6.71 (0.014)	
T2b	5.07 (0.022)	5.14 (0.027)	5.28 (0.033)	in $CHCl_3$: 4.96[e]
	5.31 (0.010)	5.41 (0.012)	5.59 (0.017)	
	5.73 (0.184)	5.84 (0.153)	6.04 (0.153)	
T4	4.22 (0.224)	4.27 (0.213)	4.44 (0.214)	in methylchloride: 4.41; 5.19[f]
	4.32 (0.037)	4.35 (0.037)	4.50 (0.039)	in dichloromethane: 4.40; 5.25[g]
	5.26 (0.427)	5.33 (0.395)	5.56 (0.409)	

[a] Ref 42. [b] Ref 43. [c] Ref 44. [d] Ref 45. [e] Ref 46. [f] Ref 47. [g] Ref 48.

bation theory up to the second-order)[24] methods for the calculation of the optimum geometry for the electronic ground state in order to analyze and discuss geometry changes induced by CN groups located at various positions in the thiophene molecule. For the obtained optimal DFT geometries, vertical excitations have been calculated using TD-DFT.[25] All computed quantities will be compared with available experimental data. Finally, for terthiophene oligomers, a detailed insight to the torsional potential energy curves for the electronic ground state and the effect of torsional potential energy curves on the absorption spectra will be presented. These investigations represent the basis for future molecular dynamics simulations of torsional broadening of the absorption and fluorescence spectra.

2. Quantum Chemical Methods

The electronic ground-state geometries of the systems with one and three thiophene rings (Figure 1) were optimized using the DFT method with the B3LYP functional.[26] MP2 calculations have been performed as a benchmark. In both cases, the 6-31G(d)[27] basis set was used. The obtained optimal geometries

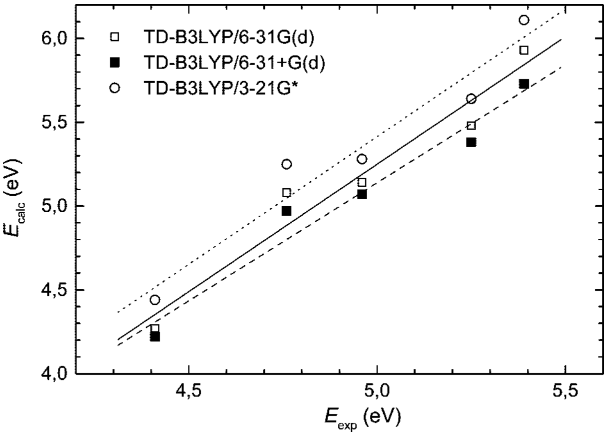

Figure 2. Correlation of theoretical TD-B3LYP/6-31G(d) electronic excitation energies with the experimental values (refs 42−47) for thiophenes.

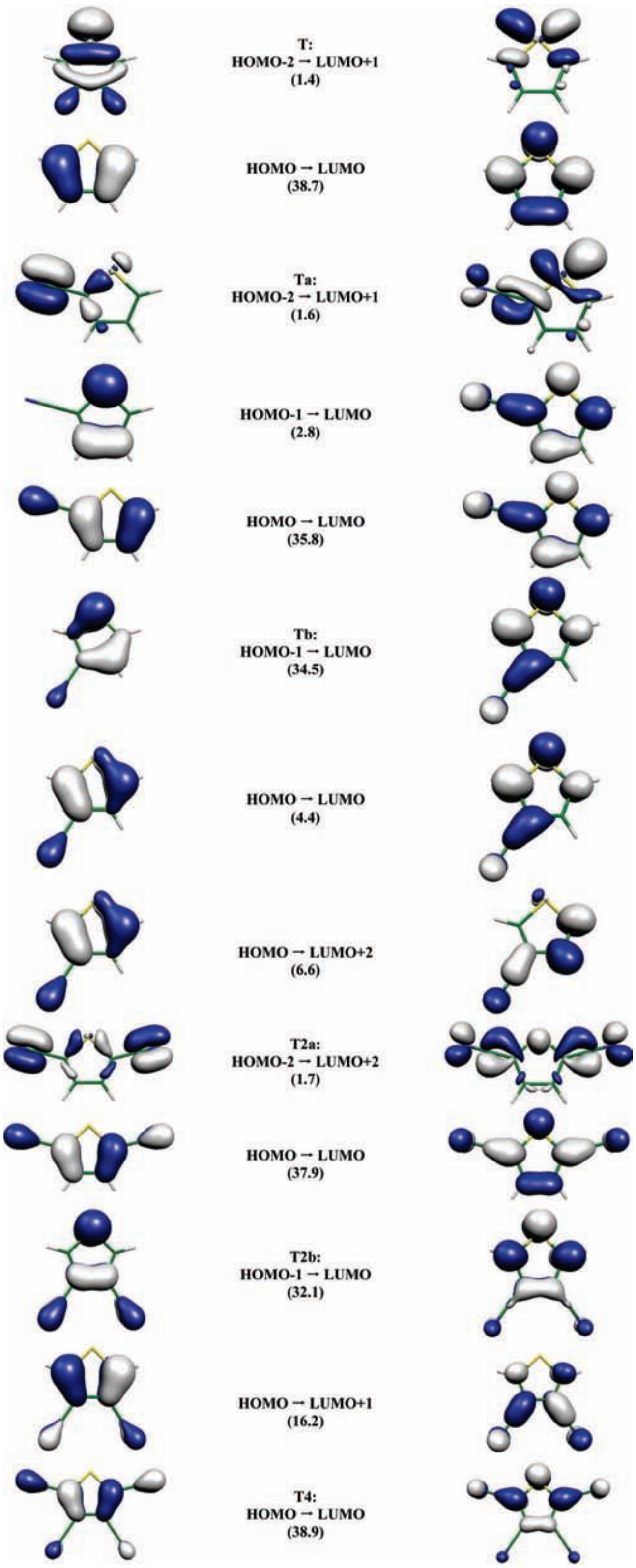

Figure 3. Plots of the B3LYP/6-31G(d) molecular orbitals significantly contributing to the lowest energy transition of thiophenes. Values in parentheses present the percentages of the excitation contributions to individual transitions.

were confirmed to be real minima by frequency calculation (no imaginary frequencies). On the basis of optimal geometries, the vertical electronic excitation energies were calculated using the time-dependent DFT approach (TD-B3LYP). The 6-31G(d), 6-31+G(d),[27] and 3-21G*[28] basis sets have been employed. All calculations were performed using the Gaussian 03 package.[29] Finally, the absorption bands in the gas phase have been simulated by sampling the configuration space with 5000 points picked from the classical harmonic oscillator approach (HOA).[30] This configuration space was obtained from the optimal B3LYP/6-31G(d) geometries (for each conformation) and their normal modes. In the case of the HOA distributions, the ensemble of geometries was generated considering constant zero-point energy at 0 K. The 10 lowest excitation energies and oscillator strengths were calculated at the TD-B3LYP/3-21G* level of theory for each fifth geometry. These quantities enabled the computation of the Einstein B coefficient. The energy of every peak was modified by a Gaussian function with the height corresponding to the Einstein coefficient and the width corresponding to an arbitrary phenomenological broadening constant (0.05 eV). The sum of all Gaussian functions plotted against the transition energy gives a post-Condon semiclassical approximation of the real spectrum. The employed approach closely follows that of ref 30 as implemented in the Newton-X package.[31]

3. Results and Discussion

3.1. Thiophenes. ***3.1.1. Structure Description.*** The obtained theoretical bond lengths for the studied thiophenes are compiled in Table 1. In the case of thiophene **T**, DFT and MP2 methods give the minimal bond lengths for bonds 2 and 4, whereas the distances between the sulfur atom and the neighboring carbon atoms (bonds 1 and 5) are the longest ones (see Figure 1). The differences between B3LYP and MP2 bond lengths are within 0.006 Å. The provided B3LYP and MP2 geometries are in good agreement with the available experimental[32,33] and theoretical MP2/TZVP data.[34] The introduction of CN substituents leads to a structure perturbation depending on the mutual position of the CN groups on the aromatic ring. Generally, bond contraction occurs for the α substitution. The largest contractions (0.015 Å for B3LYP/6-31G(d) and 0.017 Å for MP2/6-31G(d)) were found for bond 3 in molecule **T2a**. On the other hand, the prolongation of this bond was observed for CN substitutions in β positions. In the tetracyano-substituted molecule **T4**, only negligible bond length alteration of bond 3 was found.

Bond length changes in aromatic systems can be also described by bond length alternation (BLA).[35] The BLA values are defined as the differences in the average lengths of single and double bonds between non-hydrogen atoms. The positive (negative) sign of BLA indicates that the repeating unit has an aromatic (quinoid) character. As can be seen from the data in Table 1, cyano substitutions lead to lower BLA values (indicat-

TABLE 3: B3LYP/6-31G(d) and MP2/6-31G(d) Dihedral Angles (θ in deg), Ionization Potentials (IP in eV), Dipole Moments (μ_0 in D), and Total Energies (E_{tot} in hartree) of the Terthiophenes[a]

molecule (method)	conformation	optimal angles θ_1	θ_2	IP	μ_0	E_{tot}
TT:						
DFT/6-31G(d)	trans	162	−162	5.19	0.73 (0.64)	−1656.631745
MP2/6-31G(d)		144	−144	7.17	1.05 (1.00)	−1653.487012
DFT/6-31G(d)	cis	30	−30	6.06	7.58 (1.44)	−1656.629381
MP2/6-31G(d)		41	−41	7.25	1.90 (1.81)	−1653.485330
HF/6-31G(d,p)[b]	trans	149	−149			
	cis	44	−44			
TTa:						
DFT/6-31G(d)	trans	161	−161	6.04	2.64 (2.68)	−1841.115918
MP2/6-31G(d)		165	−165	8.06	3.86 (3.89)	−1837.512641
DFT/6-31G(d)	cis	26	−26	5.24	1.55 (7.75)	−1841.113393
MP2/6-31G(d)		39	−39	8.11	8.43 (8.48)	−1837.510767
TTb:						
DFT/6-31G(d)	trans	151	−151	6.05	6.93 (7.36)	−1841.115607
MP2/6-31G(d)		159	−159	8.04	7.30 (7.53)	−1837.513340
DFT/6-31G(d)	cis	31	−31	6.10	3.13 (3.46)	−1841.113700
MP2/6-31G(d)		42	−42	8.12	3.71 (3.90)	−1837.511923
TTc:						
DFT/6-31G(d)	trans	154	−154	5.78	6.86 (7.28)	−1841.112348
MP2/6-31G(d)		144	−144	7.85	7.38 (7.59)	−1837.513859
DFT/6-31G(d)	cis	23	−23	5.92	6.78 (7.28)	−1841.115414
MP2/6-31G(d)		34	−34	7.91	7.16 (7.38)	−1837.515741
TTd:						
DFT/6-31G(d)	trans	148	−148	5.96	8.02 (8.27)	−1841.109337
MP2/6-31G(d)		168	−168	7.99	8.66 (8.73)	−1837.511863
DFT/6-31G(d)	cis	23	−23	6.02	6.37 (6.79)	−1841.110707
MP2/6-31G(d)		36	−36	8.01	6.72 (6.89)	−1837.512419

[a] See Figure 1b for bond notation. Values in parentheses represent the B3LYP/6-31+G(d)//B3LYP/6-31G(d) calculations. [b] Ref 49.

TABLE 4: B3LYP/6-31G(d) and MP2/6-31G(d) Optimal Bond Lengths (in angstroms) of the Terthiophenes[a]

molecule (method)	bond	1 1′	2 2′	3 3′	4 4′	5 5′	6 6′	7 7′	8 8′	9 9′	BLA
TT:											
DFT/6-31G(d)	trans	1.735	1.368	1.424	1.379	1.757	1.448	1.756	1.379	1.417	0.196
MP2/6-31G(d)		1.719	1.378	1.415	1.386	1.734	1.448	1.734	1.387	1.409	0.176
DFT/6-31G(d)	cis	1.734	1.368	1.423	1.379	1.756	1.450	1.754	1.379	1.417	0.196
MP2/6-31G(d)		1.718	1.378	1.415	1.386	1.734	1.449	1.734	1.387	1.409	0.176
TTa:											
DFT/6-31G(d)	trans	1.751	1.380	1.413	1.384	1.751	1.445	1.754	1.381	1.413	0.189
MP2/6-31G(d)		1.729	1.388	1.407	1.389	1.732	1.446	1.734	1.389	1.407	0.171
DFT/6-31G(d)	cis	1.751	1.381	1.412	1.384	1.749	1.448	1.752	1.382	1.414	0.188
MP2/6-31G(d)		1.728	1.388	1.407	1.389	1.733	1.448	1.733	1.389	1.407	0.171
TTb:											
DFT/6-31G(d)	trans	1.723	1.378	1.432	1.375	1.759	1.449	1.753	1.379	1.416	0.194
MP2/6-31G(d)		1.710	1.386	1.420	1.384	1.734	1.448	1.732	1.388	1.408	0.173
DFT/6-31G(d)	cis	1.722	1.378	1.432	1.375	1.758	1.451	1.752	1.379	1.416	0.194
MP2/6-31G(d)		1.710	1.386	1.420	1.383	1.735	1.449	1.733	1.388	1.408	0.174
TTc:											
DFT/6-31G(d)	trans	1.734	1.362	1.434	1.393	1.750	1.448	1.752	1.385	1.409	0.191
MP2/6-31G(d)		1.717	1.373	1.423	1.396	1.731	1.446	1.732	1.392	1.403	0.173
DFT/6-31G(d)	cis	1.735	1.362	1.433	1.395	1.749	1.447	1.755	1.383	1.413	0.191
MP2/6-31G(d)		1.717	1.374	1.422	1.397	1.730	1.446	1.734	1.391	1.406	0.172
TTd:											
DFT/6-31G(d)	trans	1.728	1.370	1.417	1.384	1.758	1.446	1.753	1.387	1.445	0.191
MP2/6-31G(d)		1.715	1.379	1.411	1.390	1.732	1.445	1.730	1.394	1.427	0.172
DFT/6-31G(d)	cis	1.730	1.369	1.421	1.382	1.758	1.447	1.750	1.388	1.443	0.193
MP2/6-31G(d)		1.728	1.370	1.417	1.384	1.757	1.446	1.753	1.389	1.444	0.190

[a] See Figure 1b for bond notation.

ing a more aromatic structure). The difference between the BLA values of molecules **T** and **T4** is about 0.02 Å for the B3LYP and MP2 methods, respectively.

3.1.2. Electronic Structure and Optical Properties. Electric dipole moment and ionization potential (IP) are quantities of fundamental importance in structural chemistry. They are known to be sensitive already to small changes in the structure and the electronic charge distribution in the molecule. The calculated permanent dipole moments, μ_0, and IPs are presented in Table 1. In general, cyano substitution leads to an increase of the dipole moment. Both theoretical methods provide similar results; the differences are lower than 20%. Molecule **T2b** exhibits the maximum dipole moment. It is around 10 times larger than the dipole moment of nonsubstituted thiophene **T**. Molecules **T1a** and **T1b** exhibit approximately 7 times higher dipole moment. This is a result of the summation of CN groups contributions to the permanent dipole moment. The reliability of the theoretical results can be verified using experimental data, which are, unfortunately, available for nonsubstituted thiophene **T** only. The experimental dipole moment of 0.55[36] or 0.54 D[37] is in good agreement with our B3LYP/6-31G(d) result (0.63 D). The addition of diffuse functions, B3LYP/6-31+G(d), results in a value identical with the experimental one. MP2 gives slightly higher dipole moments for all studied thiophenes and used basis sets. The B3LYP IP values (Table 1) are by ca. 2.5 eV lower than the Hartree−Fock ones. However, experimental trends[38−41] are correctly described. The smallest IP value was found for molecule **T**. Electron-withdrawing CN groups induce an increase in IP (ca. 2 eV for **T4**).

The structural changes in the thiophene ring related to the presence of CN groups are also reflected in the vertically excited electronic states. The first three dominant vertical excitation energies are summarized in Table 2. The nonsubstituted molecule **T** exhibits the highest excitation energy. The only available experimental value for thiophene **T**, 5.39 eV in tetrahydrofurane (THF),[42] confirms a strong absorption band for the lowest energy transition. Calculated values, 5.93 eV (TD-B3LYP/6-31G(d)) and 5.73 (TD-B3LYP/6-31+G(d)), are higher by 10% and 6%, respectively. These values are in good agreement with the latest ab initio calculations of Palmer et al.[34] (5.69 eV at the CIS/QZVP level of theory).

Cyano substitutions in the thiophene ring lead to a bathochromic energy shift and to the occurrence of two dominant excitation energies. Data in Table 2 indicate that a CN group in the α position shifts the excitation energies to lower values, more than a CN group in the *β* position (see **T1a** vs **T1b** and **T2a** vs **T2b**). Besides, in compounds **T1b** and **T2b**, the CN group in the *β* position is responsible for the small intensity of the first excitation to the lowest excited state. The data presented in Table 2 indicate a strong dependence of the energies on the basis set quality. The theoretical results presented for the cyanothiophenes confirm observed experimental trends,[43−48] although the theoretical data are shifted. The correlation coefficients of calculated lowest excitation energies (E_{calc}) versus experimental energies (E_{exp}) reached 0.974, 0.971, and 0.980 for the thiophenes with the 6-31G(d), 6-31+G(d), and 3-21G* basis sets (Figure 2), respectively.

$$E_{\mathrm{calc}} = -2.36 + 1.52E_{\mathrm{exp}} \qquad \text{6-31G(d)} \qquad (1)$$

$$E_{\mathrm{calc}} = -2.20 + 1.52E_{\mathrm{exp}} \qquad \text{6-31+G(d)} \qquad (2)$$

$$E_{\mathrm{calc}} = -1.91 + 1.41E_{\mathrm{exp}} \qquad \text{3-21G*} \qquad (3)$$

In order to understand the effect of CN substituents on the absorption spectra for the lowest excitation energy, it is useful to examine the relevant (highest) occupied and lowest unoccupied molecular orbitals that play a dominant role in the electronic transitions. As can be seen in Figure 3, in all molecules, the electron is excited from the highest occupied molecular orbital (HOMO). The presented B3LYP/6-31G(d) orbitals are localized on the thiophene ring between the double bonds 2 and 4 and on the relevant CN groups. CN groups in α positions induce an around twice larger electron localization on the CN groups than the groups in *β* positions. The corresponding unoccupied orbital in this transition is the lowest unoccupied molecular orbital (LUMO). This orbital is delocalized on the sulfur atom, on the neighboring carbon atoms along the single bond 3, and on the corresponding CN groups (see Figure 3). Except for molecule **T4**, the excitations from the lower occupied orbitals (HOMO − 1, HOMO − 2) to the orbitals LUMO, LUMO + 1, or LUMO + 2 contribute by ca. 10−20% to the lowest energy transitions. These B3LYP orbitals are localized on the CN group and on the sulfur lone pair pointing in the *xy* direction (see Figure 3). We note that the respective RHF orbitals exhibit the same shape. Both the occupied and unoccupied orbitals are localized on the CN groups. Therefore, the CN group is always participating on the investigated lowest energy transitions predominantly.

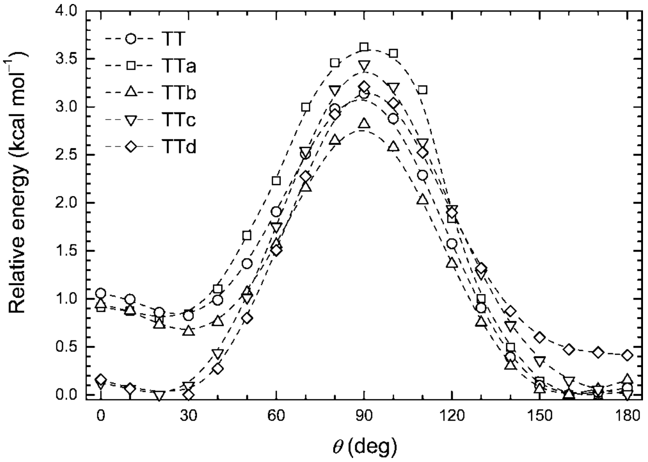

Figure 4. Dependence of the relative energy of studied terthiophenes on the torsion of one thiophene ring calculated at the B3LYP/6-31G(d) level of theory. The second dihedral angle was kept on the optimal value (see Table 3). The ground-state energy minimum represents the reference value.

3.2. Terthiophenes. ***3.2.1. Structure and Torsional Potentials.*** In comparison to the thiophenes, the studied terthiophenes exhibit a large number of conformations stemming from the presence of ring torsion around the 6 and 6′ bonds. On the basis of the previous work of Liu et al.,[49] we have restricted our calculations to the trans−trans−syn and cis−cis−syn conformations which exhibit the lowest total energies. According to the bond numbering scheme (Figure 1), the optimal dihedral angles and optimized bond lengths are compiled in Tables 3 and 4. For the nonsubstituted molecule **TT,** the B3LYP dihedral angle between the thiophene rings is 162°, whereas the MP2 method gives a value of 144°. These data are in accordance with the latest quantum chemical studies for bithiophene[50] and terthiophene,[51] where the minima were found at torsion angles between 142° and 152° for the anti conformer and between 33° and 44° for the syn conformer. Our theoretical results are also in agreement with available electron diffraction data for the bithiophene performed in the gas phase at 97−98 °C.[52] It showed the coexistence of two conformations with the inter-ring torsion angles 148° and 36°. Unfortunately, no experimental data are available for terthiophene in the gas phase. X-ray diffraction measurements showed that the oligothiophene molecules are planar in crystals.[53] For example, a 6−9° torsion angle for nonsubstituted terthiophene was observed between the external and central thiophene rings.[54]

Substitutions in various positions have a distinct effect on the dihedral angles. The trans conformations are more twisted than the cis structures. Data in Table 3 show that the CN groups located in the inner parts of the terthiophene units (**TTc** and **TTd**) stabilize the cis conformation over the trans conformation. This may represent a consequence of the sterical influence of CN groups on the inner thiophene rings, i.e., the overlap of CN with the aromatic electron distribution.

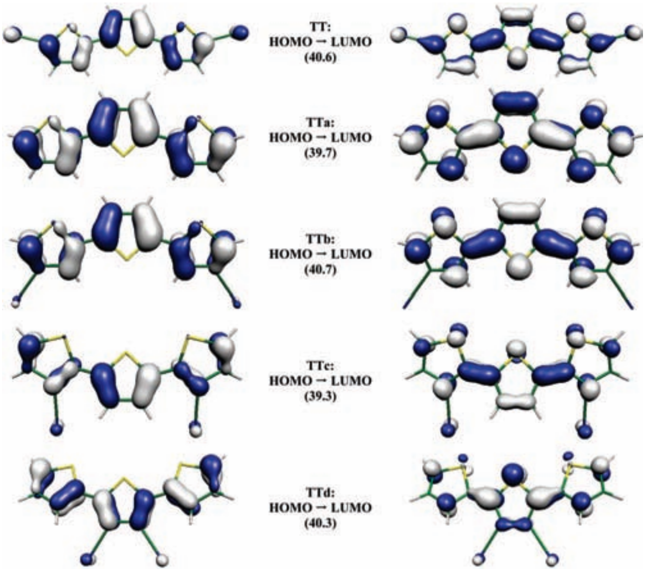

Figure 5. Plots of the B3LYP/6-31G(d) molecular orbitals significantly contributing to the lowest energy transition of terthiophenes. Values in parentheses present percentages of the excitation contributions to individual transitions.

TABLE 5: Optimum Angles (in deg) and Energy Barriers (in kcal mol^{-1}) with Respect to the Global Minima for the Terthiophenes[a]

		energy barriers		
molecule (method)	conformation	opt − 0°	opt − 180°	opt − 90°
TT:				
DFT/6-31G(d)	trans	1.058	0.072	3.140
MP2/6-31G(d)		1.687	0.734	1.882
HF/6-31G(d,p)[b]		2.115	0.452	1.864
TTa:				
DFT/6-31G(d)	trans	0.912	0.036	3.625
MP2/6-31G(d)		1.971	1.086	2.496
TTb:				
DFT/6-31G(d)	trans	0.941	0.153	2.819
MP2/6-31G(d)		1.884	1.070	2.054
TTc:				
DFT/6-31G(d)	cis	0.123	0.007	3.444
MP2/6-31G(d)		1.129	0.575	2.380
TTd:				
DFT/6-31G(d)	cis	0.161	0.411	3.213
MP2/6-31G(d)		1.056	0.918	2.086

[a] Symbol "opt" indicates the optimal angle θ_1 from Table 2. [b] Ref 49.

Comparison of the bonds between the non-hydrogen atoms, as shown in Table 4, is also quite interesting. The shortest C−C bonds in **TT** are located at the ends of the molecule (bonds 2 and 2′). Carbon−sulfur bonds, 5 and 5′, are the longest.

CN substitution leads to geometry changes in the terthiophene species. The 2 (2′), 5 (5′), and 7 (7′) bonds are elongated. The largest elongation was found for the double bond adjacent to the substituent, e.g., bond 2 in **TTa** (0.023 Å). MP2 gives slightly longer double bonds and shorter single bonds in comparison to B3LYP, but the trends in the substituent effect are analogous. The differences in the BLA values of the terthiophenes are lower (only 0.01 Å) than those found for thiophenes. This is a well-known behavior of larger aromatic systems.[35] The obtained results indicate that the effect of CN groups on the terthiophene structure is similar to the investigated thiophenes.

The electronic ground-state one-dimensional torsional potential of the terthiophenes was calculated using the B3LYP/6-31G(d) method. In the calculations, the first dihedral angle, θ_1, was changed in 10° steps, while the second one, θ_2, was kept on the optimal value (according to the data in Table 3). The obtained results are shown in Figure 4, and the barriers are summarized in Table 5. These data show the energy differences against the optimal geometry (trans conformation of **TT**, **TTa**, **TTb** and cis conformation of **TTc**, **TTd**) on dihedral angle θ. The computed curves exhibit two minima for nonplanar structures that correspond to the most stable trans or cis conformations and two first-order saddle points. The vibrational frequencies of these specific geometries were also checked using vibrational analysis. The first-order saddle point (one imaginary frequency) for the perpendicular arrangement ($\theta = 90°$) shows the highest energy barrier, whereas the planar structures represent maxima with the smallest energy barriers. Although the shapes of the presented torsional curves are comparable, the MP2 method underestimates (more than 30%) the barrier at perpendicular geometry. For example, the calculated barrier for **TT** is 1.882 kcal mol^{-1} for MP2, whereas for B3LYP it reaches 3.140 kcal mol^{-1}. The highest torsional barrier is shown by the α-substituted molecule **TTa**. On the other hand, the cyano substitution in the β position (molecule **TTb**) results in the

TABLE 6: Theoretical Excitation Energies (in eV) and Oscillator Strengths $f > 0.01$ (in Parentheses) of the First Three Dominant Electronically Excited States for the Most Stable Conformations of the Terthiophenes

	TD-B3LYP/6-31+G(d)		TD-B3LYP/6-31G(d)		TD-B3LYP/3-21G*		
molecule	trans	cis	trans	cis	trans	cis	experiment
TT	3.23 (0.760)	3.36 (0.722)	3.35 (0.799)	3.47 (0.748)	3.47 (0.821)	3.58 (0.763)	in toluene: 3.50[a]
	4.85 (0.084)	4.55 (0.019)	4.83 (0.010)	4.67 (0.016)	4.90 (0.015)	4.76 (0.014)	in ethanol: 3.53[b]
	5.46 (0.056)	4.72 (0.013)	4.98 (0.068)	4.83 (0.010)	5.09 (0.064)	4.89 (0.010)	
TTa	2.96 (1.101)	3.04 (0.982)	3.04 (1.131)	3.11 (0.998)	3.15 (1.132)	3.22 (0.999)	in toluene: 3.24[a]
	4.53 (0.051)	3.67 (0.016)	4.60 (0.044)	4.33 (0.046)	4.68 (0.049)	3.82 (0.012)	in CH_2Cl_2: 3.25[c]
	4.63 (0.014)	4.14 (0.028)	4.68 (0.013)	4.43 (0.034)	4.76 (0.010)	4.43 (0.038)	
TTb	3.29 (0.774)	3.39 (0.751)	3.38 (0.806)	3.48 (0.770)	3.49 (0.827)	3.58 (0.784)	
	4.30 (0.014)	3.88 (0.014)	4.40 (0.017)	4.47 (0.022)	4.54 (0.010)	4.67 (0.023)	
	4.79 (0.030)	4.37 (0.023)	4.56 (0.010)	4.58 (0.025)	4.65 (0.011)	4.85 (0.048)	
TTc	2.93 (0.688)	3.02 (0.754)	2.99 (0.694)	3.08 (0.759)	3.10 (0.723)	3.19 (0.778)	in toluene: 3.27[a]
	4.16 (0.010)	4.40 (0.043)	4.39 (0.020)	4.46 (0.054)	4.47 (0.032)	4.55 (0.061)	
	4.45 (0.132)	4.49 (0.058)	4.54 (0.125)	4.56 (0.045)	4.69 (0.113)	4.70 (0.041)	
TTd	3.071 (0.557)	3.15 (0.531)	3.14 (0.566)	3.21 (0.538)	3.25 (0.600)	3.32 (0.566)	in toluene: 3.32[a]
	3.67 (0.044)	3.69 (0.059)	3.72 (0.036)	3.75 (0.046)	4.31 (0.030)	4.30 (0.068)	
	4.12 (0.047)	4.13 (0.075)	4.19 (0.045)	4.19 (0.079)	4.40 (0.010)	4.50 (0.028)	

[a] Ref 20. [b] Ref 55. [c] Ref 22.

lowest energy barrier. The cyano substitution also influences the barriers for the planar structures. For example, substitution on the outer thiophene rings decreases the barrier (by about 16%) in comparison to **TT** (see opt − 0° in Table 5). A comparison of the energy difference between planar and optimal conformation, recently calculated for the molecule **TT** at the Hartree−Fock level,[49] shows a twice as large value than our B3LYP energy.

3.2.2. Electronic Structure, Optical Properties, and Absorption Spectra Simulation. The first three dominant vertical excitation energies for terthiophenes are summarized in Table 6. Generally, cyano substitution leads to a bathochromic energy shift with the exception of the *β*-substituted **TTb**. HOMO−LUMO transitions contribute dominantly to the first excitation. The orbitals in Figure 5 show the electron redistribution from double to single bonds during the excitation. In molecule **TTa**, with a CN group in α position, and in molecules **TTc** and **TTd** with CN groups in the inner ring, the HOMO and LUMO orbitals are also delocalized on the CN groups. In **TTb**, however, the CN group does not participate in the excitation. The data presented in Table 6 indicate the dependence of the excitation energies on the basis set quality. The 3-21G* basis set provides around 0.1 eV larger values than the 6-31G(d) basis set. 6-31+G(d) energies are mostly the lowest ones. The cis conformers always show larger excitation energies for the first transition. For the second transition, only the nonsubstituted **TT** and the α-substituted **TTa** cis conformers show larger energies than the trans conformers.

The dependence of the vertical excitation on the ring rotation around the single bond is quite interesting for the simulations of the absorption bands. On the basis of the geometries obtained from the B3LYP/6-31G(d) optimization, where the first dihedral angle, θ_1, was changed (in 10° steps) and the second one, θ_2, was kept on the optimal value as shown in Table 3, the lowest excitation energies were calculated. As it can be seen in Figure 6, the minima occur for the planar orientations, whereas the maxima were found for the perpendicular structures. Although the absolute values of excitation energies depend on the basis set quality, the differences between the excitation energies for the planar and perpendicular structures of the studied molecules remain constant. The smallest difference, 0.54 eV, exhibits molecule **TTd**, whereas the largest difference (0.80 eV) shows molecule **TTb**. The differences of 0.64, 0.65, and 0.68 eV were found for molecules **TTa**, **TT**, and **TTc**, respectively.

To understand the relationship between the structure and optical properties of the studied terthiophenes, the electron absorption spectra were simulated using HOA distribution. The resulting spectra are shown in Figure 7, together with the experimental spectrum of **TT**. Simulated bands in the HOA are shifted to lower energies (ca. 0.1 eV). Theoretical bands show three main peaks stemming from the vibrational flexibility of the torsion in the region from 2.8 to 3.8 eV. Our simulations also indicate that the relative intensities depend on the CN substitutions. In the case of molecule **TT**, the first peak has a lower intensity than the second and third ones. This is in agreement with the experimental observation (see the inset in Figure 7).[55] It seems that α substitution raises the intensity of the first peak, whereas substitution in the inner ring decreases the intensity of the first and third peaks. The structured shape and the shoulder appearing at longer wavelengths of the experimental absorption spectrum were also observed by Demanze et al.[20] for molecule **TTa**. The intensity of the shoulder appearing at the lowest energies (long wavelengths) decreases if CN groups are located at the inner *β* positions (**TTc** or **TTd**).

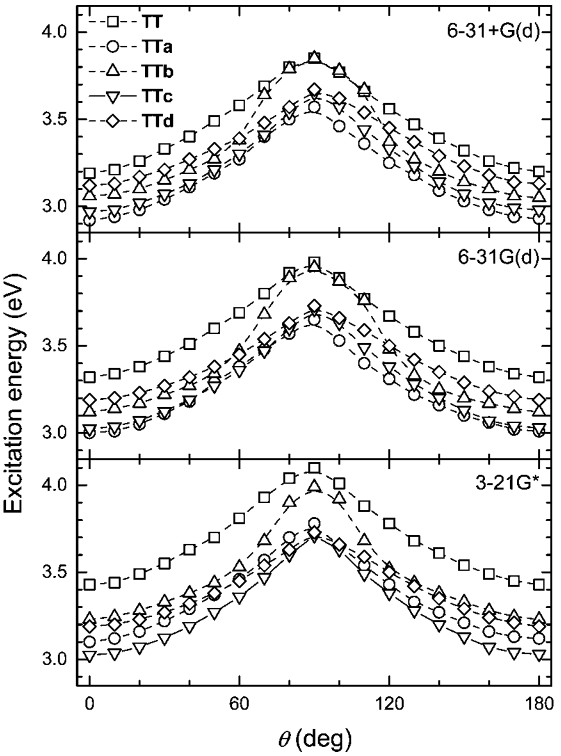

Figure 6. Dependence of the lowest excitation energy of the studied terthiophenes on the torsion of one thiophene ring based on the ground-state potential curves in Figure 4. The energies were calculated at the TD-B3LYP level of theory in three basis sets.

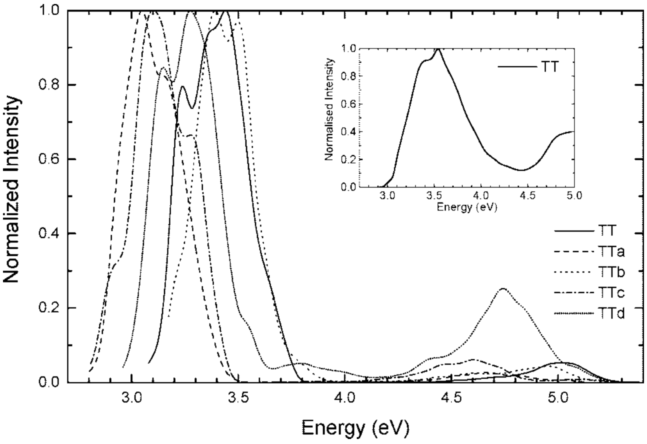

Figure 7. Simulated TD-DFT/3-21G* theoretical electron absorption spectra of terthiophenes based on the HOA distribution. Inset: Experimental absorption spectrum for **TT** (ref 55).

4. Conclusions

In this paper, electronic ground-state geometries for the selected cyano derivatives of thiophenes and terthiophenes were optimized using DFT and MP2 methods. These calculations helped to quantify the aromaticity perturbation induced by the cyano substitution. Generally, the substitutions lead to a decrease of the BLA in comparison to the nonsubstituted molecules **T** and **TT**. In the case of the terthiophenes, CN groups located in the central part of the molecule cause the preference of the cis−cis instead of the trans−trans conformation. The investigation of the B3LYP energy dependence on the torsion angle of the aromatic ring shows the highest barrier for the perpendicular arrangement for the α-substituted molecule **TTa**. On the other hand, the cyano substitution in the *β* position resulted in the lowest energy barrier for molecule **TTb**. The obtained values of dipole moments are in accordance with the expected additivity of the CN group contributions to the dipole moment.

CN groups in α and *β* positions have distinct effects on excitation energies. The calculations based on the TD-DFT approach showed that compared to nonsubstituted species, a CN group located in the α position causes a larger bathochromic shift than a CN group in the *β* position. Furthermore, a CN group in the *β* position gives rise to the narrowing of the energy range between the first three absorption bands. The nonequivalent sensitivity of the vertical excitation energies on the ring rotation around the single bond for the studied terthiophenes is also reflected in simulated absorption spectra. These simulations were based on the HOA distribution, and they indicated that a CN group in the *β* position has low influence on the position of the first absorption maximum. However, the shoulder intensity is changed. This is in agreement with the available experimental data.

Acknowledgment. This work has been supported by the Slovak Grant Agency VEGA (Project Nos. 1/3036/06 and 1/0774/08) and the Science and Technology Assistance Agency (Project Nos. APVT-20-005004 and SK-AT 00506) and by the Austrian Academic Exchange Service program Wissenschaftlich-Technische Zusammenarbeit Austria−Slovakia under contract no. ÖAD WTZ 02/2006.

References and Notes

(1) Cornil, J.; Beljonne, D.; Brédas, J. L. In *Electronic Materials: The Oligomer Approach*; Müllen, K., Wegner, G., Eds.; Wiley-VCH: Weinheim, Germany, New York, 1998; p 432.

(2) Horowitz, G.; Fichou, D.; Peng, X.; Xu, Z.; Garnier, F. *Solid State Commun.* **1989**, *72*, 381.

(3) Dodabalapur, A.; Torsi, L.; Katz, H. E. *Science* **1995**, *268*, 270.

(4) McRae, D. G.; Yamamoto, E.; Towers, G. H. N. *Biochim. Biophys. Acta* **1985**, *821*, 488.

(5) Tan, S.; Zhai, J.; Fang, H.; Jiu, T.; Ge, J.; Li, Y.; Jiang, L.; Zhu, D. *Chem. Eur. J.* **2005**, *11*, 6272.

(6) Kahol, P. K.; McCormick, B. J.; Epstein, A. J.; Pandey, S. S. *Synth. Met.* **2003**, *135*−*136*, 343.

(7) Chakraborty, D.; Lagowski, J. B. *J. Chem. Phys.* **2001**, *115*, 184.

(8) Kumar, A.; Bakhshi, A. K. *Indian J. Chem., Sect. A: Inorg., Phys., Theor., Anal.* **2006**, *45*, 352.

(9) Unver, H.; Karakas, A.; Elmali, A. *J. Mol. Struct.* **2004**, *702*, 103.

(10) Negri, F.; Zgierski, M. Z. *J. Chem. Phys.* **1994**, *100*, 2571.

(11) Breza, M.; Lukeš, V.; Vrábel, I. *J. Mol. Struct. (THEOCHEM).* **2001**, *572*, 151.

(12) Beenken, W. J. D. *Chem. Phys.* **2008**, *349*, 250.

(13) Videlot-Ackermann, C.; Isoshima, T.; Yassar, A.; Wada, T.; Sasabe, H.; Fichou, D. *Synth. Met.* **2006**, *156*, 154.

(14) Barbarella, G.; Bongini, A.; Zambianchi, M. *Macromolecules* **1993**, *27*, 2501.

(15) Garnier, F. *Angew. Chem. Adv. Mater.* **1989**, *101*, 529.

(16) Iraqi, A.; Barker, G. W.; Pickup, D. F. *React. Funct. Polym.* **2006**, *66*, 195.

(17) Cornil, J.; Dos Santos, D. A.; Beljonne, D.; Brédas, J. L. *J. Phys. Chem.* **1995**, *99*, 5604.

(18) Facchetti, A.; Yoon, M.-H.; Stern, C. L.; Katz, H. E.; Marks, T. J. *Angew. Chem., Int. Ed.* **2003**, *42*, 3900.

(19) Hapiot, P.; Demanze, F.; Yassar, A.; Garnier, F. *J. Phys. Chem.* **1996**, *100*, 8397.

(20) Demanze, F.; Cornil, J.; Garnier, F.; Horowitz, G.; Valat, P.; Yassar, A.; Lazzaroni, R.; Brédas, J.-L. *J. Phys. Chem. B* **1997**, *101*, 4553.

(21) De Oliveira, M. A.; Dos Santos, H. F.; De Almeida, W. B. *Int. J. Quantum Chem.* **2002**, *90*, 603.

(22) Guzmán, V. C.; Ortiz, R. P.; Delgado, M. C. R.; Azumi, R.; Oakley, R. T.; Casado, J.; Hernández, V.; Navarrete, J. T. L *J. Mol. Struct.* **2005**, *744*−*747*, 403.

(23) Parr, R. G.; Yang, W. *Density-Functional Theory of Atoms and Molecules in Chemistry*; Springer-Verlag: New York, 1991.

(24) Head-Gordon, M. J.; Pople, A.; Frisch, M. J. *Chem. Phys. Lett.* **1988**, *153*, 503.

(25) Stratmann, R. E.; Scuseria, G. E.; Frisch, M. J. *J. Chem. Phys.* **1998**, *109*, 8218.

(26) Becke, A. D. *J. Chem. Phys.* **1996**, *104*, 1040.

(27) Gill, P. M. W.; Johnson, B. G.; Pople, J. A.; Frisch, M. J. *Chem. Phys. Lett.* **1992**, *197*, 499.

(28) Binkley, J. S.; Pople, J. A.; Hehre, W. J. *J. Am. Chem. Soc.* **1980**, *102*, 939.

(29) Frisch, M. J.; Trucks, G. W.; Schlegel, H. B.; Scuseria, G. E.; Robb, M. A.; Cheeseman, J. R.; Montgomery, J. A., Jr.; Vreven, T.; Kudin, K. N.; Burant, J. C.; Millam, J. M.; Iyengar, S. S.; Tomasi, J.; Barone, V.; Mennucci, B.; Cossi, M.; Scalmani, G.; Rega, N.; Petersson, G. A.; Nakatsuji, H.; Hada, M.; Ehara, M.; Toyota, K.; Fukuda, R.; Hasegawa, J.; Ishida, M.; Nakajima, T.; Honda, Y.; Kitao, O.; Nakai, H.; Klene, M.; Li, X.; Knox, J. E.; Hratchian, H. P.; Cross, J. B.; Adamo, C.; Jaramillo, J.; Gomperts, R.; Stratmann, R. E.; Yazyev, O.; Austin, A. J.; Cammi, R.; Pomelli, C.; Ochterski, J. W.; Ayala, P. Y.; Morokuma, K.; Voth, G. A.; Salvador, P.; Dannenberg, J. J.; Zakrzewski, V. G.; Dapprich, S.; Daniels, A. D.; Strain, M.-C.; Farkas, O.; Malick, D. K.; Rabuck, A. D.; Raghavachari, K.; Foresman, J. B.; Ortiz, J. V.; Cui, Q.; Baboul, A. G.; Clifford, S.; Cioslowski, J.; Stefanov, B. B.; Liu, G.; Liashenko, A.; Piskorz, P.; Komaromi, I.; Martin, R. L.; Fox, D. J.; Keith, T.; Al-Laham, M. A.; Peng, C. Y.; Nanayakkara, A.; Challacombe, M.; Gill, P. M. W.; Johnson, B.; Chen, W.; Wong, M. W.; Gonzalez, C.; Pople, J. A. *Gussian 03*, revision A.1; Gaussian, Inc.: Pittsburgh, PA, 2003.

(30) Barbatti, M.; Granucci, G.; Persico, M.; Ruckenbauer, M.; Vazdar, M.; Eckert-Maksiæ, M.; Lischka, H. *J. Photochem. Photobiol., A* **2007**, *190*, 226.

(31) Barbatti, M.; Granucci, G.; Persico, M.; Ruckenbauer, M.; Lischka, H. Newton-X: A Package for Newtonian Dynamics Close to the Crossing Seam, version 0.13b, 2006; www.univie.ac.at/newtonx.

(32) Liescheski, P. B.; Rankin, D. W. H. *J. Mol. Struct.* **1988**, *178*, 227.

(33) Bak, B.; Christensen, D.; Hansen-Nygaard, L.; Rastrup-Andersen, J. *J. Mol. Spectrosc.* **1961**, *7*, 58.

(34) Palmer, M. H.; Walker, I. C.; Guest, M. F. *Chem. Phys.* **1999**, *241*, 275.

(35) Jacquemin, D.; Perpete, E. A.; Chermette, H.; Ciofini, I.; Adamo, C. *Chem. Phys.* **2007**, *332*, 79.

(36) Ogata, T.; Kozima, K. *J. Mol. Spectrosc.* **1972**, *42*, 38.

(37) Fouda, A. S. *Monatsh. Chem.* **1986**, *117*, 159.

(38) Baker, A. D.; Betteridge, D.; Kemp, N. R.; Kirby, R. E. *Anal. Chem.* **1970**, *42*, 1064.

(39) Klasinc, L.; Sabljic, A.; Kluge, G.; Rieger, J.; Scholz, M. *J. Chem. Soc., Perkin Trans. 2* **1982**, 539.

(40) Linda, P.; Marino, G.; Pignataro, S. *J. Chem. Soc. B* **1971**, 1585.

(41) Bock, H.; Roth, B. *Phosphorus, Sulfur Silicon Relat. Elem.* **1983**, *14*, 211.

(42) Inoue, S.; Jigami, T.; Nozoe, H.; Aso, Y.; Ogura, F.; Otsubo, T. *Heterocycles* **2000**, *52*, 159.

(43) Seixas De Melo, J.; Elisei, F.; Gartner, C.; Aloisi, G. G.; Becker, R. S. *J. Phys. Chem. A* **2000**, *104*, 6907.

(44) D′Auria, M. *Tetrahedron Lett.* **1995**, *36*, 6567.

(45) Sugimoto, Y.; Nishimura, S.; Imoto, E. *Nippon Kagaku Zasshi* **1961**, *82*, 1407.

(46) Levitsky, I. A.; Kishikawa, K.; Eichhorn, S. H.; Swager, T. M. *J. Am. Chem. Soc.* **2000**, *122*, 2474.

(47) Simmons, H. E.; Vest, R. D.; Blomstrom, D. C.; Roland, J. R.; Cairns, T. L. *J. Am. Chem. Soc.* **1962**, *84*, 4746.

(48) Yu, H.; Srdanov, G.; Hasharoni, K.; Wudl, F. *Tetrahedron* **1997**, *53*, 15593.

(49) Liu, F.; Zuo, P.; Meng, L.; Zheng, S. J. *J. Mol. Struct. (THEOCHEM)* **2005**, *726*, 161.

(50) Rubio, M.; Merchaìn, M.; Pou-AmeìRigo, R.; Ortiì, E. *ChemPhysChem* **2003**, *4*, 1308.

(51) Pan, J.-F.; Chua, S.-J.; Huang, W. *Chem. Phys. Lett.* **2002**, *363*, 18.

(52) Samdal, S.; Samuelsen, E. J.; Volden, H. V. *Synth. Met.* **1993**, *59*, 259.

(53) Visser, G. J.; Heeres, G. J.; Volters, J.; Vos, A. *Acta Crystallogr., Sect. B* **1968**, *24*, 467.

(54) Yassar, A.; Demanze, F.; Jaafari, A.; El Idrissi, M.; Coupry, C. *Adv. Funct. Mater.* **2002**, *12*, 699.

(55) Nivsarkar, M. *Curr. Sci.* **1999**, *76*, 1391.

JP805629U